PIER C

(Received 11 May 2024, Accepted 5 July 2024, Scheduled 18 July 2024)

Miniaturized Novel Multi Resonance Monopole Planar Antenna with Slots, Slits, Split Ring Resonator

Prasanna L. Zade* and Sachin S. Khade

Yeshwantrao Chavan College of Enginneering, Nagpur, India

ABSTRACT: The proposed multi-resonant monopole antenna has a compact design and operates between 2.9 and 6 GHz, effectively covering the full 5G sub-6 GHz spectrum (N79) as well as WLAN frequency ranges. This Miniaturized Multi-resonance Monopole Planar Antenna (MMMPA), having dimensions $25 \times 16 \times 1.6\,\text{mm}^3$ ($L \times W \times h$), is ideally suited for wireless communication devices and systems. The antenna achieves triple resonances, encompassing the frequency bands from 2.9 to 6 GHz, through an inventive construction consisting of rectangular patch, U slots, key-shaped slots, split ring resonators, and annular rings forming an electromagnetic band-gap (EBG) structure. A strong degree of agreement and correlation amongst the simulation and measurement findings attests to the antenna's dependable operation. Even though the patch size was reduced by around 65% with reference to referred geometry.

1. INTRODUCTION

Over the years, significant research efforts have been dedicated to develop compact, simple structure, minimal weight, and cost-efficient antennas for various wireless communication applications. Planar antennas are one of the various types of antennas and have drawn the most attention because of its inherent benefits. However, they also suffer from certain limitations, such as low gain, low power management capacity, and narrow bandwidth when operating at with miniaturized dimensions [1, 2].

This size reduction technique is preferred in most of the wireless compact devices. Planar antennas are known for their compact and low-profile design, making them suitable for integration into various wireless devices, such as smartphones, tablets, wearables, and internet of things (IoT) devices [9–11].

Their planar structure can be designed to operate over a wide range of frequencies, enabling support for multiple communication standards and bands, and play a vital role in providing reliable and high-speed wireless connectivity. The careful selection of shape, dimensions, and positions of slots and slits is instrumental in disturbing radiation pattern of the patch, effectively creating a broad impedance bandwidth and improved overall antenna efficiency [2–4].

2. ANTENNA DESIGN AND SIMULATION

The proposed final design of antenna geometry is shown in Fig. 1. It shows optimized dimensions of patch, slots, slits, partial ground plane, SRR and EBG structure. The antenna is designed on FR4 substrate having dimensions $25 \times 16\,\text{mm}^2$. The patch is feed by Microstrip feed line.

The proposed antenna structure is simulated by using CST Studio. The evolution of antenna is done in five stages as depicted in Fig. 2.

Comparative analysis of simulated results for all evolutions is depicted in Fig. 3. Fig. 2(a) shows the 1st evolution's radiating patch and ground plane respectively with the dimensions of $38 \times 30\,\text{mm}^2$, resulting in single ultra-wideband response with resonant frequency at 4.43 GHz and bandwidth of 990 MHz. Fig. 2(b) illustrates the altered configuration in the second stage of development, featuring the addition of two U-shaped slots with inverted uneven stepped slits positioned beneath the radiating patch, as well as on the top of the partial ground plane, along with a slit on back side of the feed line located at the center of partial ground plane [5, 6]. This led to an uneven current distribution on both sides of the patch, a setup that can be adjusted to generate an additional band when the antenna dimensions are reduced to $32 \times 27\,\text{mm}^2$, resulting in dual bands at frequencies 4.5 GHz and 5.5 GHz. Band 1 shows narrow band response with a bandwidth of 140 MHz, while Band 2 showcases a considerably broader bandwidth of 920 MHz. The strategic placement of slots and slits on the radiating patch significantly influences antenna performance [17]. Incorporating double U-slots onto the patch yields a multi-band response. Through precise positioning of these slots, the desired resonance frequency bands can be finely tuned and attained.

In order to use the same antenna for additional applications in wireless bands, antenna geometry is further modified by adding key-shaped slots on radiating patch along with a wider slit at the center of ground plane as shown in Fig. 2(c), so it alters the effective electrical size of the ground plane, which influences the antenna's resonant frequency and radiation pattern. The dimensions of 3rd evolution of antenna patch is further reduced to $30 \times 25 \times 1.6\,\text{mm}^3$. The use of partial ground planes alters the effective permittivity of the substrate and ground plane region, resulting in the reduction in effective permittivity and leads to a decrease in the physical size for the same resonance at a given frequency. The main focus of this patch is to enhance the performance in terms targeted multi-band and size re-

* Corresponding author: Prasanna L. Zade (zadepl@gmail.com).

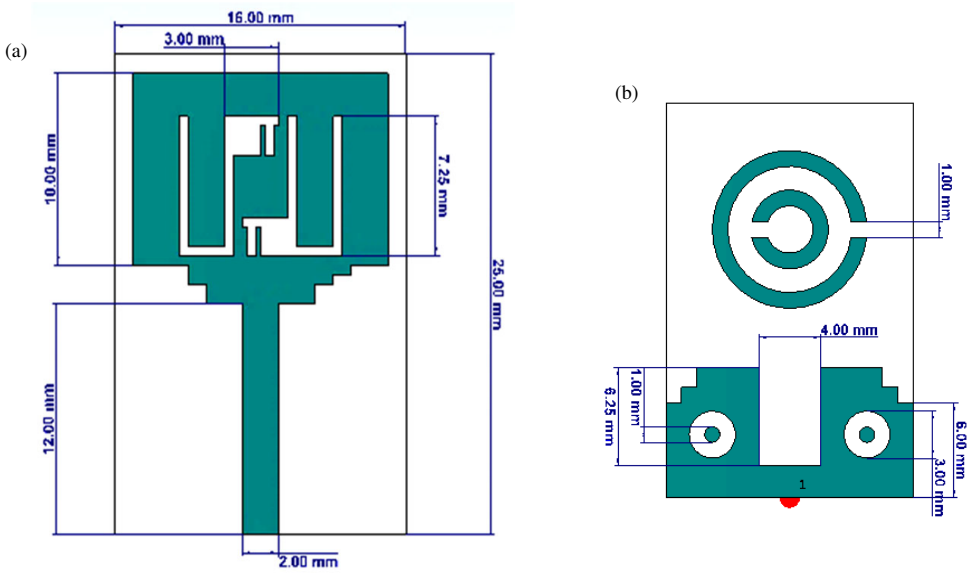

FIGURE 1. (a) Radiating patch of proposed MMMPA. (b) Ground plane of proposed MMMPA.

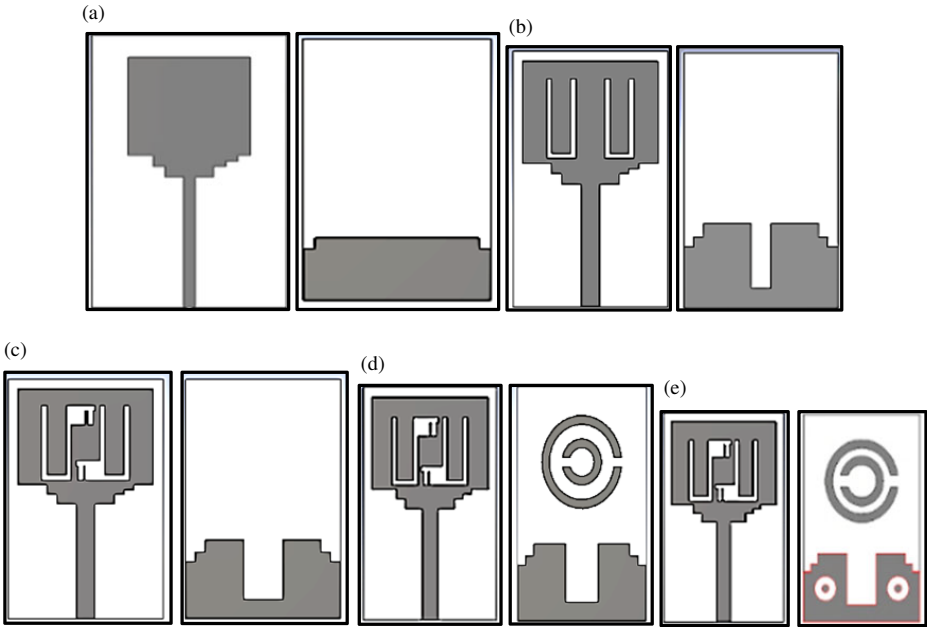

FIGURE 2. Evolution of proposed antenna design (five Stages). (a) Radiating patch. (b) Ground plane.

duction [13, 19]. Also, 3rd resonance and corresponding bands are introduced at frequencies 4.5 GHz, 5.5 GHz, and 5.8 GHz with corresponding return losses -21.18 dB, -22.92 dB, and -15.25 dB, respectively.

U-slot technique is a widely used method in microstrip design for achieving multi-band operation. To achieve more than two frequency bands, incorporating double U-slots within the radiating patch is essential. A basic microstrip antenna is often modeled as a parallel combination of resistance, inductance, and capacitance, denoted as C_1, L_1, and R_1, respectively, as defined in

$$C_1 = \frac{\varepsilon_0 \varepsilon_{eff}}{2h} LW \cos -2\left(\frac{\pi y_o}{L}\right) \tag{1}$$

y_o is the feed coordinate

$$L_1 = \frac{1}{w^2 C_1} \tag{2}$$

$$R_1 = \frac{Q_r}{wC_1} \tag{3}$$

$$Q_r = C\frac{\sqrt{\varepsilon_{eff}}}{4fh} \tag{4}$$

Figure 4(a) depicts a conceptual design highlighting a U-slot loaded patch, and it can be examined through the conceptualization of two distinct sections [5]. In Part 1, two parallel notches are integrated, causing a modification in the current path length.

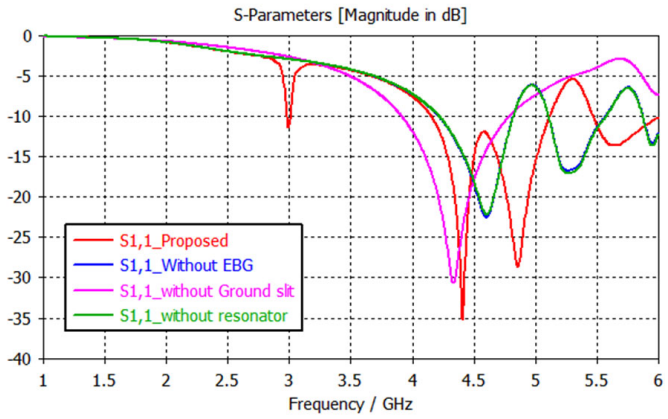

FIGURE 3. Comparison of Simulated results of Evolution's.

This modification is facilitated by incorporating additional series capacitance and inductance into the parallel equivalent of lumped resistance, capacitance, and inductance elements. Part 2 considering two microstrip curve lines, with the equivalent impedance of this configuration expressed as a series inductance combined with a parallel inductance and capacitance arrangement for each of the microstrip curved lines [14]. The equivalent circuit for Part 1 is depicted in Fig. 4(b), where a series inductance, ΔL_1, is introduced to augment L_1, resulting in:

$$L_2 = L_1 + 2\Delta L_1 \tag{5}$$

and a series capacitance, $\Delta C1$, is added to $C1$ to become:

$$C_2 = \frac{C_1 \Delta C_1}{C_1 + \Delta C_1} \tag{6}$$

The equivalent circuit of Part 2 is composed of two microstrip bend lines. Each bend line can be represented by the following transmission line model Fig. 4(b), where

$$\frac{C_b}{W_b} = (9.5\varepsilon_r + 1.25)\frac{W_b}{h} + 5.2\varepsilon_r + 7.0\,\text{PF/m} \tag{7}$$

$$\frac{2L_b}{h} = 100\left[4\sqrt{W_b/h} - 4.21\right]\,\text{nH/m} \tag{8}$$

Incorporating split ring resonators (SRRs) into the ground plane not only offers antenna size reduction but also offers an antenna frequency tuning and harmonic suppression [18]. Fig. 4(c) indicates the equivalent circuit of U slot loaded patch.

Figure 2(d) illustrates the fourth stage of evolution of the proposed antenna, wherein split ring resonators are embedded in the ground plane beneath the radiating patch. This implementation aims to enhance the magnetic coupling between the patch and the rings at resonance, thereby improving efficiency, bandwidth, and further reducing the overall dimension of the antenna.

The projected antenna features a partial ground plane to effectively cover the targeted frequency bands at 2.9 GHz, 4.5 GHz, 4.9 GHz, and 5.6 GHz, appropriate for various wireless applications. Additionally, the overall dimensions of the antenna have been further minimized. Fig. 2(e) depicts the ultimate iteration of the proposed antenna design, which features a square patch loaded with double U slots and double key-shaped slots, accompanied by a partial ground plane incorporating inverted stepped shape slits. The geometry is further enhanced with the addition of split ring resonators and an annular ring shape (EGB) structure within the ground plane [7, 8].

Improved bandwidth is achieved at the expense of reduced circuit performance due to higher losses as the quality factor drops. Consequently, a trade-off must be made between the values of L and C so as to maintain the antenna's performance [16].

The impact of the slot, slit, SRR, EBG, and defected ground structure (DGS) on the proposed antenna performance has been analyzed through simulation and testing, allowing for alterations to achieve the desired characteristics. The proposed antenna has a radiating patch with dimensions of $25 \times 16\,\text{mm}^2$. The insertion of a partial ground plane with a defected ground structure serves to enhance the bandwidth by reducing surface wave current and radiation leakage. Annular rings with a thickness of 1 mm are introduced onto the ground plane, positioned on either side of the central slit. This action elongates the current path, consequently leading to an increase in inductance and a decrease in capacitance due to the greater distance between the patch and ground plane. This adjustment facilitates frequency tuning to the desired value. Consequently, an enhancement in gain to an optimal level has been observed across various frequency bands.

The design of split ring resonators (SRRs) serves to facilitate the attainment of targeted frequency responses and size reduction while maintaining performance integrity. These resonators shape the electromagnetic fields, thereby enhancing antenna efficiency. Through careful adjustment of the size and positioning of these resonators, the radiation characteristics of modifications are possible for microstrip patch antennas, including beam steering and beam shaping. Above their initial resonance, SRR exhibits a high diamagnetism, behaving as a resonator that can be stimulated by an external magnetic flux [12]. The SRR resonance frequency is provided by $(L_s C_s)^{-1/2}/2\pi$, where $C_s = C_o/4$ is the series capacitance of SRR, $C_0 = 2\pi r_0 C^*$, where C^* is the capacitance per unit length in-between the rings.

Figure 5 depicts the design of the SRR alongside its corresponding equivalent circuit model. The inductance, denoted as L_s, can be estimated by approximating that of a single ring with radius of r_0 and a ring width of c. In Fig. 6, simulated results are presented, showcasing the return loss plotted against frequency. Furthermore, the voltage standing wave ratio (VSWR) values at all desired resonances remain within the range of 1 to 2.

The antenna achieves a multi-band response with a maximum gain of 2.56 dB (directivity 3.27 dBi). The antenna resonates at frequencies 2.97 GHz, 4.45 GHz, 4.86 GHz, and 5.65 GHz, with corresponding bandwidths of 200 MHz, 972 MHz, and 460 MHz, as depicted in Fig. 6.

The corresponding return loss is -11.56 dB, -37.68 dB, -29.33 dB, and -13.67 dB at respective resonances. These

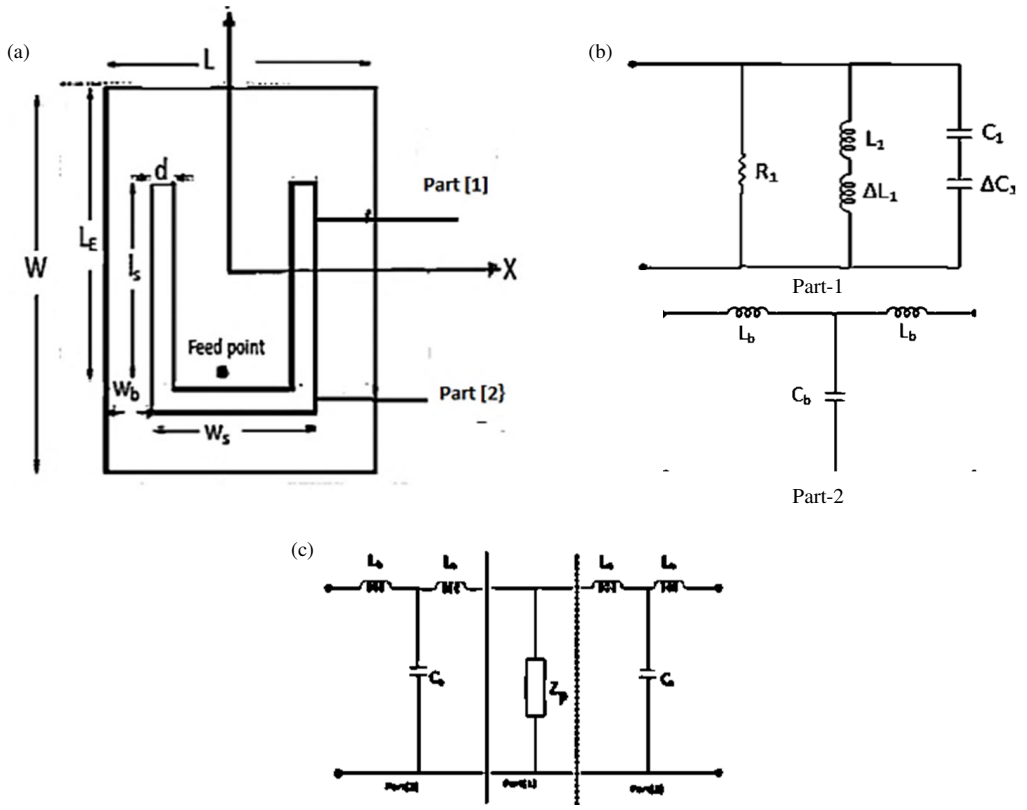

FIGURE 4. Lumped element equivalent circuits. (a) U-slot configuration. (b) Lumped element equivalent circuits. (c) Equivalent circuit of U slot loaded patch.

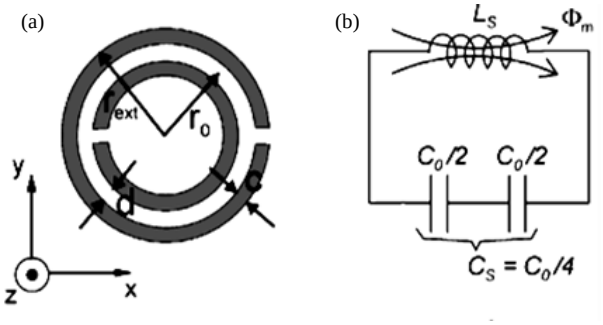

FIGURE 5. (a) SRR and (b) equivalent-circuit models.

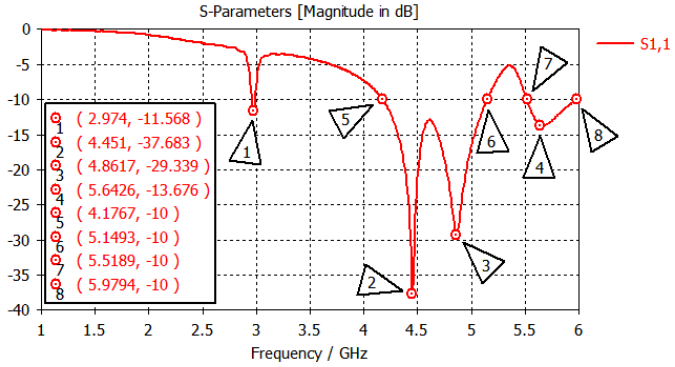

FIGURE 6. Return loss of 5th evolution proposed antenna.

frequency bands are utilized for various applications such as Wi-Fi, Short-Range Radar, Satellite Uplinks/Downlinks, and WLAN. Incorporating the rectangular patch with an EBG structure has expanded the antenna's bandwidth and reduced its size compared to the antenna without an EBG [15].

Table 1 outlines the modifications from the 1st to the 5th evolution, presenting a comparison in terms of resonance bands, antenna size, and bandwidths.

The antenna radiation patterns plays a crucial role in optimizing the design and performance evaluation, ensuring that the antenna meets the specific requirements of its intended application. The radiation pattern provides insight into the gain (directivity) and how the implemented antenna radiates or receives the signal in a particular plane, whether horizontal or vertical. Fig. 7 shows the simulated 2D and 3D radiation patterns of the antenna at frequencies 2.9 GHz, 4.5 GHz, 4.9 GHz, and 5.65 GHz, respectively. The investigated antenna's gain, directivity, radiation efficiency, 3 dB beam-width, and bandwidth are illustrated at the desired frequencies in Table 2.

The obtained radiation pattern is symmetric, bidirectional, and relatively stable across the operating frequency bands. Hence, our proposed antenna design structure behaves like a monopole antenna, with radiation being bidirectional in the elevated plane and omnidirectional in the azimuth plane. Parametric analysis plays a crucial role in microstrip antenna design to optimize performance. The antenna's performance has been studied to improve bandwidth, gain, and radiation characteris-

TABLE 1. Parametric analysis.

Evolutions	Freq. bands	Band Width (MHz)	Area mm^2	Modifications on Patch and Ground
1st	4.43	990	$38 \times 30 = 1140\,\text{mm}^2$	Introduce stepped size slits at the bottom of the patch and Partial ground
2nd	4.5 & 5.5	140 & 920	$32 \times 27 = 864\,\text{mm}^2$	Introduce Double U slots and slit at the center of ground plane
3rd	4.5, 5.5 & 5.8	175, 900& 320	$30 \times 25 = 750\,\text{mm}^2$	Introduce Double Key shaped slots and wider slit at the center of ground plane
4th	2.9, 4.5, 4.9 & 5.64	200, 972 & 460	$28 \times 20 = 560\,\text{mm}^2$	Introduce SRR
5th	2.9, 4.5, 4.9, 5.64	200, 972, & 460	$25 \times 16 = 400\,\text{mm}^2$	Introduce annular ring shaped EGB

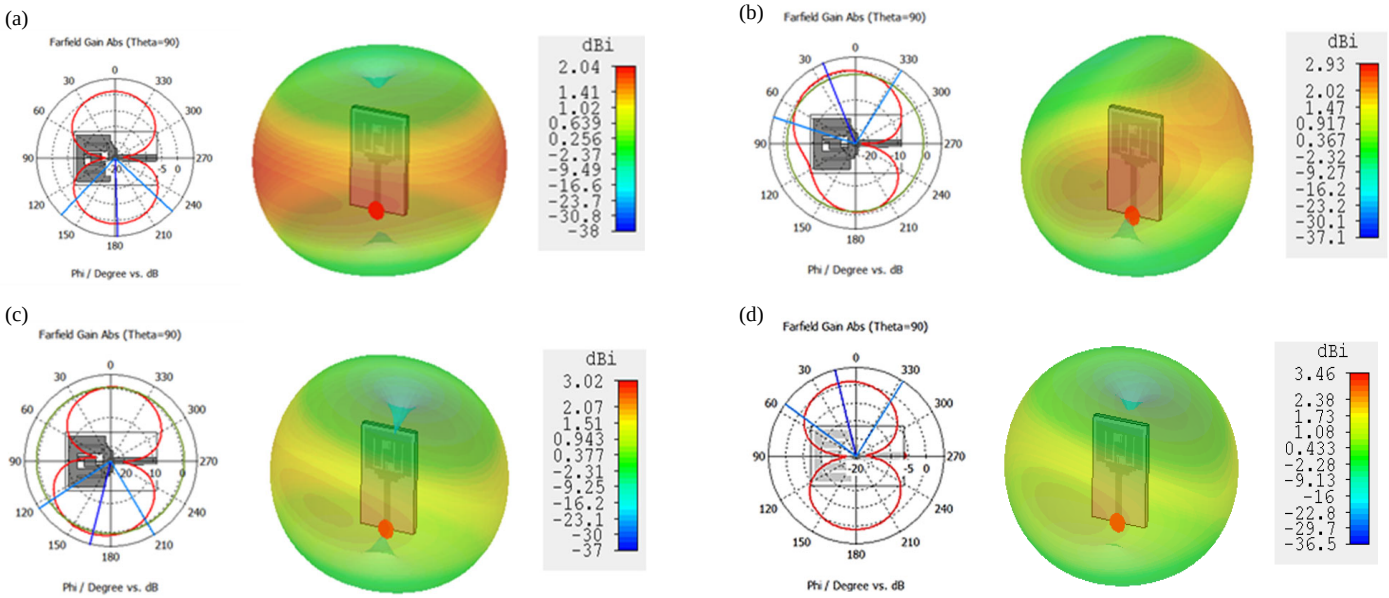

FIGURE 7. 2D and 3D radiation patterns (far field gain) at (a) 2.9 GHz, (b) 4.5 GHz, (c) 4.9 GHz and (d) 5.64 GHz.

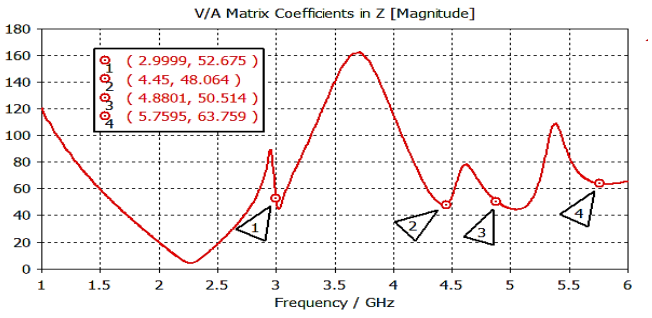

FIGURE 8. Input impedance magnitude variation w.r.t frequency.

tics by adjusting the dimensions of slots, split ring resonators (SRRs), and electromagnetic band gap (EBG) structures.

It has been observed that increasing the width of the double U slots leads to frequency tuning, causing the first frequency band to shift to a lower frequency, while the remaining frequency bands remain unchanged with a slight increase in gain.

Increasing the spacing between the two split rings leads to a decrease in capacitance effects. This decrease results in the appearance of new resonances, allowing for multiple bands to be tuned at the targeted frequency while reducing the size and improving the antenna gain. Moreover, adjusting the spacing between the openings of the split ring resonator (SRR) enhances efficiency.

Figure 8 shows impedance plot, i.e., $Z_{in}(\Omega)$ vs frequency (GHz). Optimal impedance matching is achieved when the impedance curve at the resonant frequency closely approaches 50 Ω.

Figure 8 clearly illustrates the input impedance curve approaching 50 Ω impedance with respect to resonance bands, thereby enabling maximum power transmission across the pro-

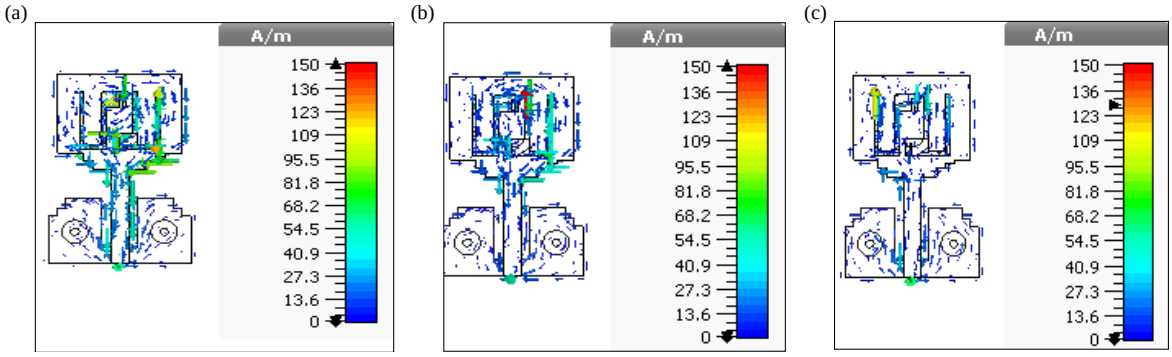

FIGURE 9. Surface current distribution. (a) $f = 2.9$ GHz. (b) $f = 4.5$ GHz. (c) $f = 5.64$ GHz.

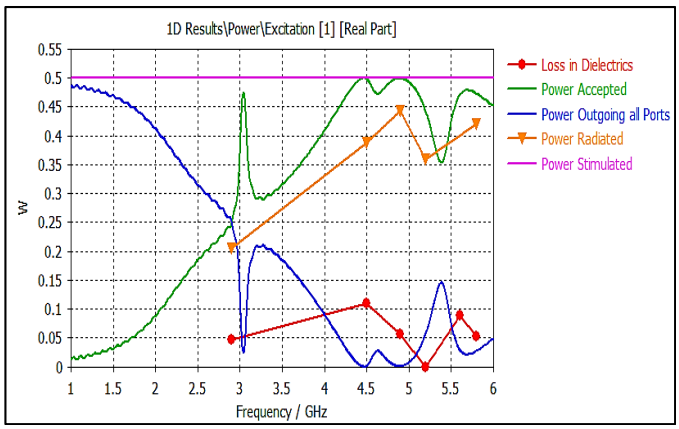

FIGURE 10. The power pattern analysis.

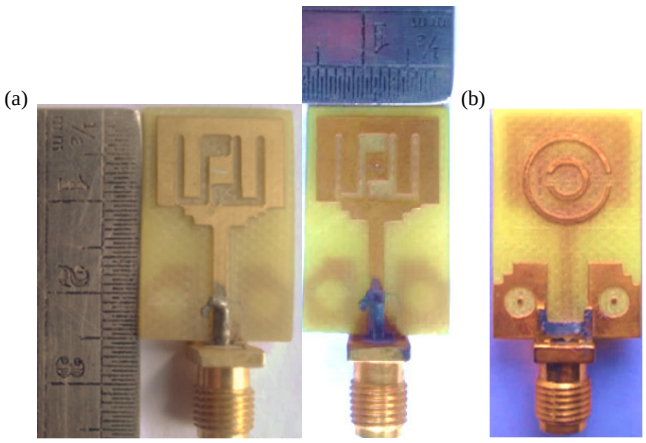

FIGURE 11. Implemented antenna design. (a) Front view. (b) Back view.

TABLE 2. Parametric results of antenna.

Frequency GHz	Gain (dBi)	Radiation Efficiency (%)	3 dB Beam Width	Band Width MHz
2.9	2.18	82.2	90.5°	120
4.5, 4.9	2.93, 3.02	78.5, 89	104.4°, 84.9°	980
5.6	3.27	90	89.2°	460

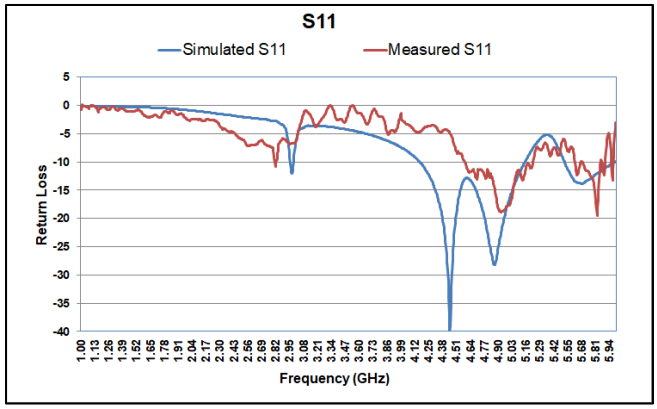

FIGURE 12. Comparison of simulated and measured result of return loss of 5th (final) evolution.

posed operating bands. The surface current circulation of the 5th evolution planar antenna at the desired resonance frequencies is indicated by Fig. 9.

The excitation of surface waves on the substrate can degrade the performance of microstrip antennas. The information of surface wave current distribution helps in designing planar antennas to get the necessary impedance matching. The slots and slits can be strategically placed for the frequency tuning and to decrease the excitation of surface waves to operate the microstrip antenna at a specific frequency band operation. The power pattern analysis, as shown in Fig. 10, indicates the antenna accepting the power over the 2.5 GHz to 6 GHz as denoted by the green line. The most of accepted power is then radiated, with only minimal power loss, indicating the high efficiency attained by the proposed antenna. The radiation efficiency varies in the range of approximately 78% to 90%.

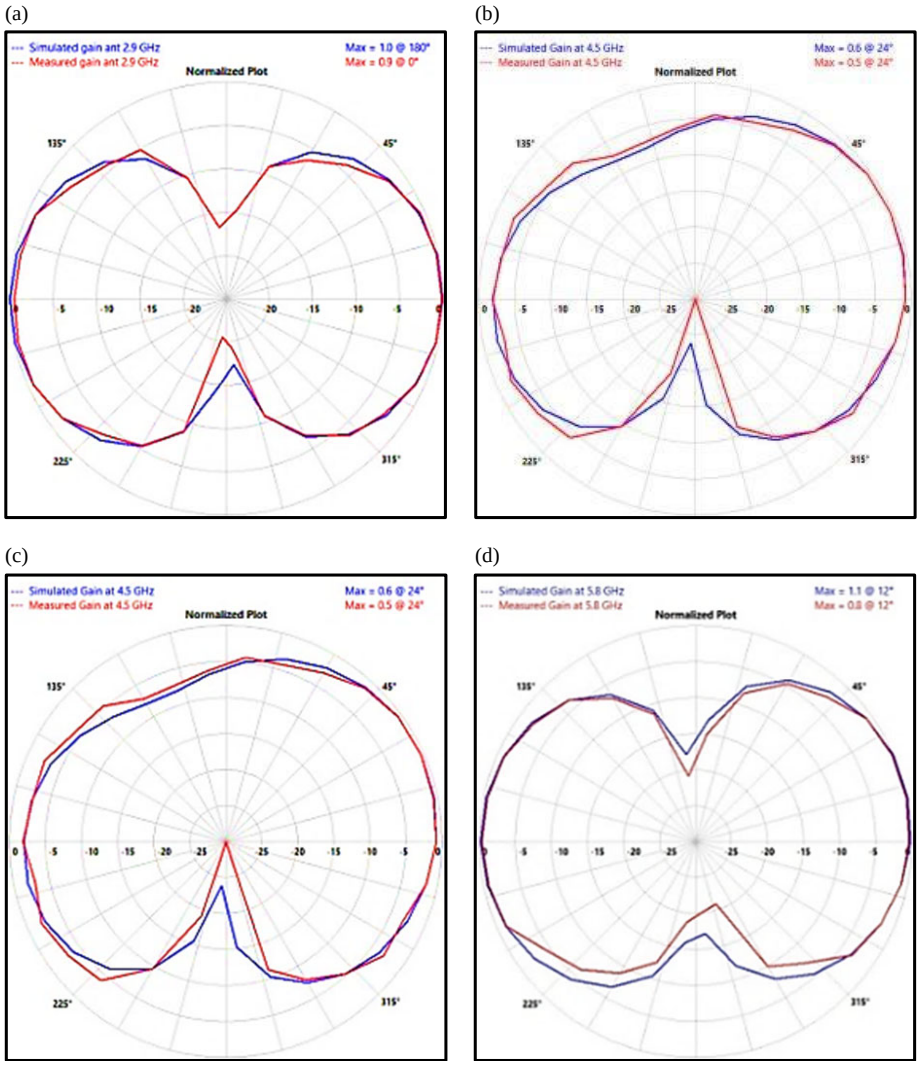

FIGURE 13. Measured and simulated E plane radiation patterns (far field gain). (a) 2.9 GHz. (b) 4.5 GHz. (c) 4.9 GHz. (d) 5.8 GHz.

TABLE 3. Comparison of proposed antenna with previous work.

Sr. No.	Referred antenna	Dimension $(W \times L \times H)$ mm^3	Frequency Band	Maximum Gain (dBi)	Efficiency
1	Proposed design	$25 \times 16 \times 1.6$	4.72 GHz to 5.24 GHz	2.18 to 3.28	78% to 90%
2	5	$46 \times 46 \times 1.6$	1.8, 2.4 and 3.5 GHz	2.6	71%
3	8	$19 \times 25 \times 1.6$	2.0–2.76, 3.04 to 4.0, 5.2 to 6.0 GHz	1.5 to 3.13	87% to 92%
4	9	$36 \times 40 \times 1.6$	6.11 GHz	5.04	77%
5	10	$29 \times 19 \times 2$	5.1 GHz	-	79%
6	16	$40 \times 40 \times 0.8$	3.28–3.54 and 8–10.85 GHz	2.5	80%
7	19	$20 \times 17 \times 1.575$	26.98–29.55 GHz	8.5	84.5%

3. ANTENNA DESIGN AND IMPLEMENTATION

A prototype of a multi-resonance antenna is fabricated and measured to validate the simulation results. The proposed design prototype is depicted in Fig. 11. Fabrication of the prototype for the miniature monopole multiband microstrip antenna (MMMPA) is carried out using a CNC engraving machine, and the prototypes are tested using a VNA.

Figure 12 presents a comparison of the suggested antenna's measured and simulated scattering characteristics. The simulated findings and measured S-parameter data have been ob-

served to correlate extremely well. The measured results are little bit deviated from the simulated ones, due to the losses across the dielectric material. We know the losses across the FR4 increases with increase in frequency.

To conduct radiation pattern measurements, we utilized an antenna measurement system and compared the obtained E-plane patterns with the simulated ones. Fig. 13 depicts the compared radiation patterns at (a) 2.9 GHz, (b) 4.5 GHz, (c) 4.9 GHz, and (d) 5.8 GHz frequencies. The correlation appears relatively high at the frequency of 4.5 GHz.

4. COMPARISON WITH PREVIOUS WORK

The performance of the proposed multiple resonance antennas is compared with previous works. The significance of proposed antenna is highlighted in terms of number of bands, size reduction, and antenna gain. Earlier works give dual bands with less antenna gains of 1.11 dBi and 1.71 dBi whereas the proposed antenna gives three bands with gains of 2.18 dBi, 3.0 dBi, and 3.28 dBi at three resonances with reduction on size by 65% as compared to earlier works. Table 3 specifies the comparison of proposed work with previous works.

5. CONCLUSION

A new design for a miniature multi-resonance monopole planar antenna (MMMPA) has been introduced. The effects of incorporating double U slots and a key-shaped slot on the radiating patch, as well as integrating a split ring resonator (SRR) and electromagnetic band gap (EBG) structure with a partial ground plane, have been investigated. The characteristics of these antennas have been examined through simulation and verified by fabricated structure results. The antennas exhibit three resonances with satisfactory gain and bandwidth, while also achieving a reduction in size by 65%. The maximum gain attained by the antenna is 3.28 dBi with an efficiency of 90%. Excellent agreement between experimental and theoretical results has been demonstrated.

REFERENCES

[1] Balanis, C. A., *Antenna Theory: Analysis and Design*, 2nd ed., John Wiley & Sons, New York, 1997.

[2] Kumar, G. and K. P. Ray, *Broadband Microstrip Antennas*, Artech House, Boston, London, 2002.

[3] Garg, R., P. Bhartia, I. Bahl, and A. Ittipiboon, *Microstrip Antenna Design Handbook*, Artech House, Boston, London, 2001.

[4] Bahl, J. J. and P. Bhartia, *Microstrip Antennas*, 355, Artech House, Jan. 1980.

[5] Ata, O. W., M. Salamin, and K. Abusabha, "Double U-slot rectangular patch antenna for multiband applications," *Computers & Electrical Engineering*, Vol. 84, 106608, Jun. 2020.

[6] Mandal, S., A. Karmakar, H. Singh, S. K. Mandal, R. Mahapatra, and A. K. Mal, "A miniaturized CPW-fed on-chip UWB monopole antenna with band-notch characteristics," *International Journal of Microwave and Wireless Technologies*, Vol. 12, No. 1, 95–102, 2020.

[7] Ekke, V. and P. Zade, "Implementation of EBG configuration for asymmetric microstrip antenna to improve radiation properties," *Journal of Telecommunication, Electronic and Computer Engineering (JTEC)*, Vol. 9, No. 1, 61–66, 2017.

[8] Gautam, A. K., L. Kumar, B. K. Kanaujia, and K. Rambabu, "Design of compact F-shaped slot triple-band antenna for WLAN/WiMAX applications," *IEEE Transactions on Antennas and Propagation*, Vol. 64, No. 3, 1101–1105, Mar. 2016.

[9] Raval, F., Y. P. Kosta, and H. Joshi, "Reduced size patch antenna using complementary split ring resonator as defected ground plane," *AEU — International Journal of Electronics and Communications*, Vol. 69, No. 8, 1126–1133, 2015.

[10] Zhang, Q.-L., Y.-T. Jin, J.-Q. Feng, X. Lv, and L.-M. Si, "Mutual coupling reduction of microstrip antenna array using metamaterial absorber," in *2015 IEEE MTT-S International Microwave Workshop Series on Advanced Materials and Processes for RF and THz Applications (IMWS-AMP)*, Suzhou, China, Jul. 2015.

[11] Deshmukh, A. A. and K. P. Ray, "Analysis of shorted-plate compact and broadband microstrip antenna," *IEEE Antennas and Propagation Magazine*, Vol. 55, No. 6, 100–113, Dec. 2013.

[12] Limaye, A. U. and J. Venkataraman, "Size reduction in microstrip antennas using left-handed materials realized by complementary split-ring resonators in ground plane," in *2007 IEEE Antennas and Propagation Society International Symposium*, 1869–1872, Honolulu, HI, USA, 2007.

[13] Elsadek, H. and D. M. Nashaat, "Multiband and UWB V-shaped antenna configuration for wireless communications applications," *IEEE Antennas and Wireless Propagation Letters*, Vol. 7, 89–91, 2008.

[14] Sudhakar, A., M. Satyanarayana, M. S. Prakash, and S. K. Sharma, "Single band-notched UWB square monopole antenna with double U-slot and key shaped slot," in *2015 Fifth International Conference on Communication Systems and Network Technologies*, 88–92, Gwalior, India, 2015.

[15] Kokotoff, D. M., R. B. Waterhouse, and J. T. Aberle, "An annular ring coupled to a shorted patch," *IEEE Transactions on Antennas and Propagation*, Vol. 45, No. 5, 913–914, May 1997.

[16] Kulkarni, J., C.-Y.-D. Sim, R. Talware, V. Deshpande, A. Chitre, and J. Anguera, "Design and analysis of dual band tapered-fed monopole antenna for 5G and satellite applications," in *2021 IEEE 18th India Council International Conference (INDICON)*, 1–6, Guwahati, India, 2021.

[17] Saleh, C. M., E. Almajali, S. S. Alja'afreh, and J. Yousaf, "Dual U-slot patch antenna for 5G applications," in *2021 IEEE International Symposium on Antennas and Propagation and USNC-URSI Radio Science Meeting (APS/URSI)*, 349–350, Singapore, 2021.

[18] Zade, P., P. Jumle, and S. Khade, "Miniaturized high bandwidth microstrip antenna using metamaterial concept based technology," in *2021 International Conference on Computational Performance Evaluation (ComPE)*, 556–559, Shillong, India, Dec. 2021.

[19] Paul, L. C., M. H. Ali, N. Sarker, M. Z. Mahmud, R. Azim, and M. T. Islam, "A wideband rectangular microstrip patch antenna with partial ground plane for 5G applications," in *2021 Joint 10th International Conference on Informatics, Electronics & Vision (ICIEV) and 2021 5th International Conference on Imaging, Vision & Pattern Recognition (icIVPR)*, 1–6, Kitakyushu, Japan, 2021.